chains. It is also our intention to perform X-ray crystallography measurements at high static pressure to study the pressure effects on the crystal lattice in these materials and to assess the relaxation effects that take place when pressure is released.

Acknowledgment. We thank Robert R. Ryan, Carol J. Burns, and Don T. Cromer for helpful discussions. This work was performed under the auspices of the U.S. Department of Energy with support from the Office of Basic Energy Sciences, Materials Science Division, and the Center for Materials Sciences of Los Alamos National Laboratory.

Supplementary Material Available: Tables of intensity data for determining the crystal system of **1** and anisotropic thermal parameters for **1** and **2** (2 pages); tables listing structure factors for **1** and **2** (3 pages). Ordering information is given on any current masthead page.

Contribution from the Departments of Chemistry and Biophysics, University of Rochester, Rochester, New York 14642, and Squibb Institute for Medical Research, P.O. Box 191, New Brunswick, New Jersey 08903-0191

Nuclear Magnetic Relaxation in Aqueous Solutions of the Gd(HEDTA) Complex

Griselda Hernandez,[†] Harry G. Brittain,[§] Michael F. Tweedle,[§] and Robert G. Bryant*[,‡]

Received April 5, 1989

The luminescence decay times and rate constants of terbium complexed with HEDTA (*N*-(2-hydroxyethyl)ethylenediaminetriacetic acid) are obtained at pH values ranging from pH 1.5 to 12 and used to determine the number of water molecules bound at the inner coordinate sphere of the lanthanide complex. The proton nuclear magnetic relaxation rate, $1/T_1$, is reported as a function of pH for gadolinium complexed with HEDTA over a range of magnetic field strengths corresponding to proton Larmor frequencies between 0.01 MHz and 30 MHz. The data analysis is largely based on the Solomon, Bloembergen, and Morgan equations after the outer-sphere contribution is taken into account. The number of water molecules in the first coordination sphere was measured by using fluorescence lifetime methods and the assumption that the result is the same for the lanthanide complex of gadolinium and terbium. The parameters obtained from the analysis are consistent with other estimates of interatomic distances and rotational correlation times. Further, the data show that the dimerization of the complex at high pH does not compromise the relaxation efficiency of the metal center, but it increases approximately by a factor of 2.

Control of magnetic relaxation holds promise for important applications in medical imaging and diagnosis. Further, if the relaxation is coupled to specific chemistry, the control of relaxation may provide a remote reporter of localized organ function using conventional magnetic imaging methods. Of the several classes of magnetic relaxation agents,[1-3] paramagnetic metal complexes provide excellent relaxation efficiency as well as a very rich chemistry that permits considerable flexibility in the control of reagent delivery in vivo. Ions with long electron spin relaxation times are most efficient affectors of nuclear spin relaxation. For paramagnetic centers with short electron relaxation times, the dominant contribution to the correlation time for the electron–nuclear coupling may be the electron relaxation itself. If this relaxation time is shorter than rotational or exchange correlation times, the efficiency of the paramagnetic center for nuclear relaxation is limited. For very short electron spin relaxation times, the dominant effect may be a large induced chemical shift rather than relaxation.[4-6] Thus, attention has focused on the atoms with S state electronic structures such as manganese(II) and gadolinium(III). Many of the clinically interesting complexes are based on chelating agents comprised largely of carboxylate groups such as EDTA or DTPA.[7] Though these complex ions appear to be very simple, their chemistry may be complicated by structural and electronic changes as a function of the complex ion dynamics or structure, which may be altered by pH or the apparent viscosity of the medium. In the present report we focus on the pH dependence of the water proton spin relaxation in aqueous solutions of Gd(HEDTA), which was chosen because aggregation of this complex has been demonstrated at alkaline pH values and thus provides a convenient approach to quantitative assessment of the relaxation effects associated with bringing two paramagnetic centers very close together.

Experimental Section

Nuclear magnetic relaxation measurements were made on a field-cycling spectrometer that switches magnetic field strengths in real time from values limited by Earth's magnetic field to a proton Larmor frequency of 42 MHz using a field controller and passing stage built at the IBM Watson Laboratories in the laboratory of Dr. Seymour Koenig.[8-11] Three Sorensen SRL-60-35 power supplies operated in parallel provide the main current source, supplemented by a capacitor bank and a secondary power supply for rapid field switches. The system employs a copper-wound solenoid bathed in liquid nitrogen to handle the heat dissipation. The probe is a single saddle coil inductor mounted at the end of a rigid coaxial line that forms a component of the resonant probe circuit, the remaining capacitive elements of which reside outside the magnet and cryostat. A simple parallel tuned circuit is used that is matched with a single series capacitor.

The radio frequency spectrometer derives the resonance frequency from a crystal oscillator at 21 or 7.25 MHz, which is amplified after a Vari-L rf SS-30 rf gate by an ENI 10-W broad-band amplifier. The receiver is protected in the usual way with series-crossed diodes on the transmitter side and crossed diodes to ground at the input to the Meiteq preamplifier located one-fourth of a wavelength from the transmitter insertion. The preamplifier is followed by an Avantek 502-515 series cascade that operates into a Merrimack doubly balanced mixer where the reference is typically set 300 kHz from the resonance frequency. The resulting demodulated signal at 300 kHz is then detected with an absolute value detector to yield an audio signal that is amplified and filtered by using a homemade system.

In a typical experiment the spins are first brought to a proton resonance frequency of 30 MHz and polarized there for a period of $5T_1$. The field is then switched to a value of interest for a variable time, τ, after

* To whom correspondence should be addressed at the Biophysics Department, University of Rochester Medical Center, Rochester, NY 14642.
† Department of Chemistry, University of Rochester.
‡ Departments of Chemistry and Biophysics, University of Rochester.
§ Squibb Institute for Medical Research.

(1) Brasch, R. C. *Radiology* **1983**, *147*, 781.
(2) Wolf, G. L.; Joseph, P. M.; Goldstein, E. J. *Am. J. Radiol.* **1986**, *147*, 367.
(3) Koenig, S. H.; et al. *Invest. Radiol.* **1986**, *21*, 697.
(4) Dwek, R. A. *Nuclear Magnetic Resonance in Biochemistry, Applications to Enzyme Systems*; Clarendon: Oxford, England, 1973.
(5) La Mar, G. N., Horrocks, W. D., Holm, R. G., Eds. *NMR of Paramagnetic Molecules*; Academic: New York, 1973.
(6) Bertini, I.; Luchinat, C. *NMR of Paramagnetic Molecules in Biological Systems*; Benjamin/Cummings: Menlo Park, CA, 1986.
(7) Lauffer, R. B. *Chem. Rev.* **1987**, *87*, 901.
(8) Redfield, A. G.; Fite, W., II; Blerch, H. E. *Rev. Sci. Instrum.* **1968**, *39*, 710.
(9) Hallenga, K.; Koenig, S. H. *Biochemistry* **1976**, *15*, 4255.
(10) Brown, R. D.; Brewer, C. F.; Koenig, S. H. *Biochemistry* **1977**, *16*, 3883.
(11) Fukushima, E.; Roeder, S. B. W. *Experimental Pulse NMR, A Nuts and Bolts Approach*; Addison-Wesely Publishing Co., Inc.: Reading, MA, 1981.

0020-1669/90/1329-0985$02.50/0

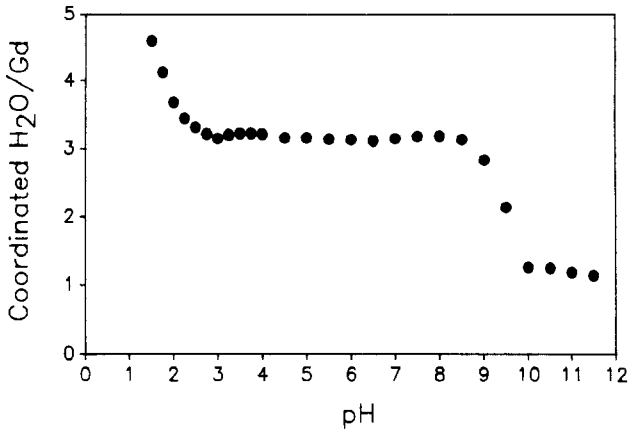

Figure 1. pH dependence of the number of first coordination sphere water molecules for the Gd(HEDTA) complex determined by luminescence analysis of the analogous Tb(HEDTA) complex.

which the field is switched to the resonance field (7.25 or 21 MHz) where a single 90° pulse is applied to create a free-induction decay. A sample-and-hold circuit is activated to capture the amplitude of the signal, which is digitized by an IBM 9094 device coupler that ties the spectrometer to an IBM 5120 computer. A series of 16, 24, or 32 τ values are used for each relaxation time determination and the data fit with a nonlinear least-squares procedure. The statistical errors are typically about 1%. Samples are contained in 10-mm Pyrex test tubes stoppered with rubber stoppers and screw caps. Temperature is maintained by a flow of liquid perchloroethylene that is thermostated in an external Neslab RTE-8 temperature controller, which services the sample region of the nitrogen cryostat with outboard Little Giant pumps.

HEDTA and $GdCl_3$ were used as received from Aldrich Chemical Co., while hydrated $TbCl_3$ was used as received from Research Chemicals. Stock solutions were prepared by the dissolution of appropriate quantities of material, and the solutions were prepared by mixing stoichiometric amounts (1:1 mole ratio) of the stock solutions. For the luminescence experiments, a final Tb(III) concentration of 10 mM was used. The ionic strength of the solutions was not controlled.

The pH of each solution was varied between pH 1.5 and 12, with the required photophysical measurements being obtained at each pH value. Variation of the solution pH of each solution was effected by the addition of microliter amounts of standard NaOH or HCl directly to the cuvette. The pH was measured using a glass microcombination electrode which could be directly inserted into the cuvette. The pH meter was calibrated daily by using phosphate buffers.

Luminescence lifetimes of the Tb(HEDTA) solutions were obtained by exciting the samples with the pulsed 337-nm output of a nitrogen laser (Model LN-1000, Photochemical Research Associates) and capturing the decay curve on a boxcar averager (Model SR-265, Stanford Research Associates). The luminescence decay times and rate constants were obtained by fitting the decay curve to a single exponential function.

Results and Discussion

It is now well established that the number of water molecules bound at the inner coordination sphere of a lanthanide complex may be determined by evaluating the magnitude of the deuterium isotope effect in luminescence lifetimes.[12,13] The data obtained on Tb(HEDTA) are shown in Figure 1, where the pH dependence of the hydration state is illustrated. HEDTA begins to bind to Tb(III) above pH 1, and full formation of the Tb(HEDTA) complexes causes the number of coordinated water molecules to drop from approximately 8 (aquo ion) to around 3. This species persists up to pH 8.5, where the number of coordinated waters decreases again, finally leveling off at 1 by pH 10. This latter species remains stable up to pH 11.5.

The trends in coordinated solvent molecules coordinate excellently with the known coordination chemistry of lanthanide HEDTA complexes. By the use of energy transfer from Tb(HEDTA) donor to Eu(HEDTA) acceptor species, it has been shown that the complexes are capable of existing either as monomer or oligomer units.[14] Between pH 3 and 8.5, lanthanide

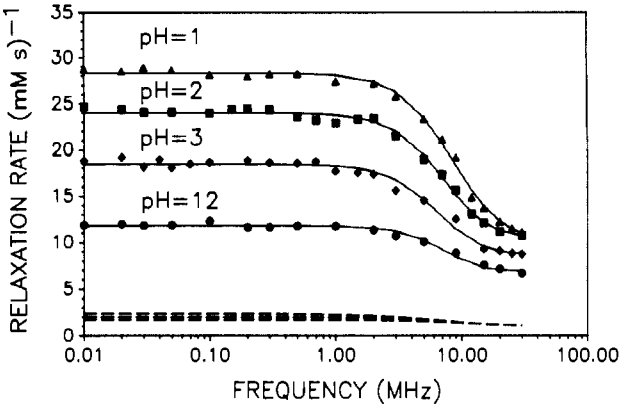

Figure 2. Water proton nuclear magnetic spin–lattice relaxation rate as a function of the magnetic field strength plotted as the proton Larmor frequency of 1 mM aqueous Gd(HEDTA) at 25 °C. Each curve represents a different pH value. The solid lines fitting the experimental data are the sum of the inner- and outer-sphere contributions; the inner-sphere contribution was calculated by using the Solomon, Bloembergen and Morgan equation and the outer-sphere contribution calculated by using Freed's equation, assuming b = 5 Å and $D = 3 \times 10^{-5}$ cm^2 s^{-1}. The dashed lower curves are the outer-sphere contribution.

HEDTA complexes exist as monomers, but above pH 9 they self-associate into oligomer units. Potentiometric titration evidence[15] strongly indicates that the oligomers are in fact μ-hydroxy-bridged species, probably dimeric in nature.

Measurements of the water proton nuclear magnetic relaxation dispersion profile were made from pH 1 to 12 for aqueous Gd(HEDTA) solutions. Representative data are shown in Figure 2 as the relaxation rate per millimole of gadolinium plotted as a function of the proton Larmor frequency in MHz. Several features are immediately apparent.

The water in the sample is uniformly affected by the paramagnetic center as expected from the rapid exchange of water between the first coordination sphere and the bulk. This classic exchange averaging[16-19] is summarized by

$$1/T_1 = q\{[\mathrm{Gd(III)}]/[\mathrm{H_2O}]\}/(T_{1m} + \tau_{ex}) + 1/T_1^\circ \qquad (1A)$$

where q is the number of water-coordinated molecules per gadolinium ion, the square brackets denote molar concentration, T_{1m} is the relaxation time, τ_{ex} is the mean residence time for the water protons in the first coordination sphere of the metal complex, and T_1° is the diamagnetic contribution. Solomon, Bloembergen, and Morgan have described the relaxation in the first coordination sphere for S state ions as[17,20,21]

$$1/T_{1m} = \{(2/15)\gamma_I^2\gamma_s^2 S(S+1)/r^6\}\{3\tau_{c1}/(1+\omega_I^2\tau_{c1}^2) + 7\tau_{c2}/(1+\omega_s^2\tau_{c2}^2)\} + (2/3)S(S+1)(A/\hbar)^2\tau_{2e}/(1+\omega_s^2\tau_{2e}^2) \qquad (1B)$$

where γ_I and γ_s are the nuclear and electron magnetogyric ratios, ω_I and ω_s are the Larmor frequencies for the nuclear and electron spins, $\hbar$ is Planck's constant divided by 2π, r is the distance from the metal center of a hydrated ion to a proton of hydration, S is the spin of the paramagnetic ion, A is the electron–proton hyperfine coupling constant, and the correlation times are given by eqs 2 and 3, where τ_{rot} is the rotational correlation time of the

$$\tau_{ck}^{-1} = \tau_{rot}^{-1} + \tau_{ex}^{-1} + \tau_{sk}^{-1} \qquad k = 1, 2 \qquad (2)$$

$$\tau_{2e}^{-1} = \tau_{ex}^{-1} + \tau_{s2}^{-1} \qquad (3)$$

(12) Horrocks, W. D., Jr.; Sudnick, D. R. *J. Am. Chem. Soc.* **1979**, *101*, 334.
(13) Brittain, H. *Nucl. Med. Biol.* **1988**, *15*, 17.
(14) Spaulding, L.; Brittain, H. G. *Inorg. Chem.* **1983**, *22*, 3486.
(15) Prados, R.; Stadtherr, L. G.; Donato, H.; Martin, R. B. *J. Inorg. Nucl. Chem.* **1974**, *36*, 689.
(16) Zimmerman, J. R.; Brittin, W. E. *J. Phys. Chem.* **1957**, *61*, 1328.
(17) Bloembergen, N.; Morgan, L. O. *J. Chem. Phys.* **1961**, *34*, 842.
(18) Swift, T. J.; Connick, R. E. *J. Chem. Phys.* **1962**, *37*, 307.
(19) Luz, Z.; Meiboom, S. *J. Chem. Phys.* **1963**, *40*, 2686.
(20) Solomon, I. *Phys. Rev.* **1955**, *99*, 559.
(21) Bloembergen, N. *J. Chem. Phys.* **1957**, *27*, 572.

Table I. Relaxation Parameters[a]

pH	coordinated H_2O/Gd	$10^{11}\tau_R$, s	$10^{11}\tau_v$, s	$10^{19}B$, s^{-2}	r, Å
1	4.6	3.2	1.2	6	2.8
2	3.7	4.3	1.4	11	2.8
3	3.1	5.1	1.6	11	2.9
12	1.1	5.7	1.6	21	2.6

[a] These fitting parameters are based on eq 1–5 after subtracting the computed outer-sphere relaxation rate contribution based on eq 6A and 6B.

intermoment vector, τ_{ex} is the mean lifetime of the nucleus in the paramagnetic environment, and τ_{s1} and τ_{s2} are the electron spin longitudinal and transverse relaxation times, respectively. The electron relaxation times are generally dependent on the magnetic field strength. This dependence may be complicated because a number of interactions may contribute to shifts in the electron resonance frequency and the electron relaxation rates.[22-24] We assume here the simplest model[17,24-26] for the electron relaxation rates given by eqs 4 and 5, where B is a constant proportional to

$$1/\tau_{s1} = B\tau_v[1/(1 + \omega_s^2\tau_v^2) + 4/(1 + 4\omega_s^2\tau_v^2)] \quad (4)$$

$$1/\tau_{s2} = B\tau_v[1.5 + 2.5/(1 + \omega_s^2\tau_v^2) + 1/(1 + 4\omega_s^2\tau_v^2)] \quad (5)$$

the strength of the interaction driving relaxation, which is assumed to be the zero-field splitting in most cases, and τ_v is a correlation time that modulates this interaction. These equations neglect any contribution from the electron–metal nucleus hyperfine coupling that may contribute to a spread of electron resonance frequencies.[27,28] The electron spin resonance line width of these complexes has been measured at the concentrations used in these nuclear relaxation studies and found to be considerably in excess of the anticipated hyperfine splittings for gadolinium complexes. Thus, neglect of this contribution to the relaxation equation is justified.

The data of Figure 2 do not have any obvious contribution from the scalar term, which usually is apparent as a low-frequency inflection.[29] This result is consistent with the expectation that the electron–proton hyperfine coupling constant, A, should be very small for lanthanide complexes since the f electrons are thought to be well screened from the bonding interactions.[30,31] The absence of a low-frequency inflection caused by the scalar term could also arise in the event that the electron relaxation rate was very large. However, if this were the case, the relaxation efficiency of the complex would be reduced for the dipolar term as well, which is not observed.

The dispersion curves fall into three classes: those for pH values less than 3, those for pH values between 3 and 9, and those for pH values between 10 and 12. The four distinctive profiles obtained are shown in Figure 2. The order of the curves shown in Figure 2 is consistent with the idea that with increasing pH an increasing number of water molecules are displaced as the ligand binds to the metal. Once the complex is formed, the relaxation rate is essentially independent of pH until pH values around 10 where an association reaction changes the structure of the complex and additional protons are removed.

The analysis of magnetic relaxation in metal complexes of this sort requires quantitative inclusion of contributions from the outer coordination sphere of the paramagnetic center. This problem has been examined in detail elsewhere[32,33] where it was concluded

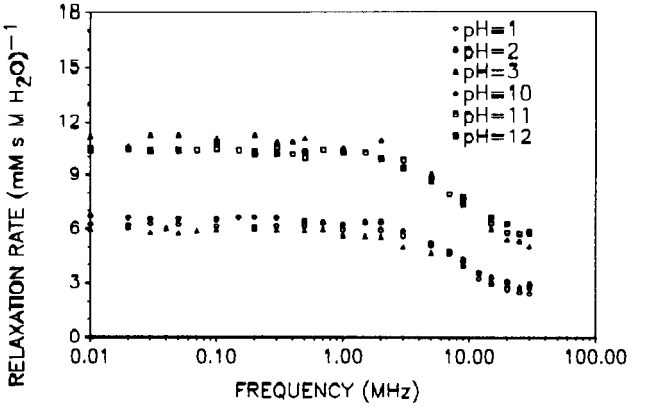

Figure 3. Water proton nuclear magnetic spin–lattice relaxation rate as a function of the magnetic field strength plotted as the proton Larmor frequency of 1 mM aqueous Gd(HEDTA) normalized to the number of water molecules coordinated to the metal center at 25 °C. The three upper curves are at pH 1, 2, and 3; the three lower curves are at pH 10, 11, and 12.

that the outer-sphere contribution to relaxation will be dominated by the transitional motion of the water in the vicinity of the paramagnetic center. This fact permits the outer-sphere contribution and the field dependence to be computed with the assumption that the translational mobility of the solvent is perturbed little in the vicinity of the complex ion, an assumption that is supported by an earlier study.[33] The outer-sphere contribution is then given by[34]

$$1/T_1 = (32\pi/405)\gamma_I^2\gamma_S^2\hbar^2S(S + 1)(Na/1000)([S]/bD) \times \{j_2(\omega_s - \omega_I) + 3j_1(\omega_I) + 6j_2(\omega_s + \omega_I)\} \quad (6A)$$

with the spectral density function $j_k(\omega)$

$$j_k(\omega) = \mathrm{Re}\{[1 + s/4]/[1 + s + 4s^2/9 + s^3/9]\} \quad (6B)$$

$$s = b\{(i\omega + (\tau_{sk})^{-1})/D\}^{1/2} \qquad k = 1, 2$$

where b is the distance of closest approach between the centers of the molecules on which the I and S spins are located, D is the relative translational diffusion coefficient given by $D = D_I + D_S$ where D_I and D_S are the individual diffusion constants of the molecules containing the I and S spins, τ_{sk} is the S spin relaxation time as given by eqs 4 and 5, Re means the real part of the expression, and the other terms are the same as in eq 1. Substitution of $^7/_2$ for S, 3×10^{-5} cm^2 s^{-1} for D, and 5 Å for b leads to the relaxation dispersion contribution shown in Figure 2 as the dashed lines. It is clear that, for the monomer units, the outer-sphere relaxation is not a major contribution to the relaxation profile, though there is a contribution to the high-frequency region apparent. We note that, in the dimer case, the outer-sphere contribution will be attenuated somewhat by the fact that the electron relaxation rate decrease will also affect the apparent correlation time for the outer-sphere dipole–dipole coupling.

The solid curves shown in Figure 2 were computed by using eqs 1–3 after the outer-sphere contribution had been accounted for with the assumption that the diffusion constant for water does not change in the vicinity of the complex ion.[33] These data are described well by a Lorentzian function. Thus, regardless of the additional details, the assumption that the correlation function decays exponentially is adequate. For the samples below pH 9, the correlation times and intermoment distances obtained are reasonable, and they are summarized in Table I for different pH values. This summary is not meant to imply that eq 1 is entirely sufficient to describe the data accurately at all frequencies; however, with the exception of the samples above pH 10 to be addressed later, nothing unusual is required of the intermoment distances in the complex or the correlation times to compute a line through the data points. The values listed in Table I are

(22) Gregson, A. K.; Dodrell, D. M. *Pegg, D. T. Aust. J. Chem.* **1978**, *31*, 469.
(23) Poupko, R.; Baram, A.; Luz, A. *Mol. Phys.* **1974**, *27*, 1345.
(24) Kowalewski, J.; Nordenskiold, L.; Benetis, N.; Wostlund, P. O. *Prog. Nucl. Magn. Reson. Spectrosc.* **1985**, *17*, 141.
(25) McLachlan, A. D. *Proc. R. Soc. London, A* **1964**, *280*, 271.
(26) Rubinstein, M.; Baram, A.; Luz, Z. *Mol. Phys.* **1971**, *20*, 67.
(27) Bertini, I.; Briganti, F.; Koenig, S. H.; Luchinat, C. *Biochemistry* **1985**, *24*, 6287.
(28) Banci, L.; Bertini, I.; Briganti, F.; Luchinat, C. *J. Magn. Reson.* **1986**, *66*, 58.
(29) Koenig, S. H.; and Brown, R. D., III. *Magn. Reson. Med.* **1984**, *1*, 478.
(30) Koenig, S. H.; Epstein, M. *J. Chem. Phys.* **1975**, *63*, 2279.
(31) Koenig, S. H.; Baglin, C.; Brown, R. D., III. *Magn. Reson. Med.* **1984**, *1*, 496; **1986**, *3*, 242.
(32) Polnaszeck, C. F.; Bryant, R. G. *J. Chem. Phys.* **1984**, *81*, 9, 4038.
(33) Lester, C. C.; Bryant, R. G. *J. Phys. Chem.*, in press.
(34) Freed, J. H. *J. Chem. Phys.* **1978**, *68*, 4034.

consistent with the correlation time for the dipolar term being dominated by the rotational correlation time for the complex ion since values for the rotational correlation time are expected to be in the several tens of picoseconds range.[35,36]

The data of Figure 2 are shown again in Figure 3 normalized to the number of water molecules bound to the metal at each pH value. It is now clear that the data fall into only two classes, those below pH 10 and those pH 10 and above. The relaxation dispersion data for samples with pH between 3 and 9 are coincident with pH 3. These data show that the relaxation efficiency of the metal center remains essentially unchanged as the monomeric complex is formed. This observation is consistent with the effective correlation time for the electron-nuclear coupling being that for rotation. However, the relaxation efficiency increases significantly when additional water is displaced by the association reaction even though the metal centers are brought close together in the dimer.

It is likely that the high pH product is predominantly a dimer of the μ-hydroxo or μ-oxo type previously reported for EDTA complexes.[37] The properties of transition-metal dimers and their magnetic relaxation properties in particular have been discussed by several groups.[38-40] One might assume that the relaxation rate in the dimer should double because each proton in the bridging position may interact with two electron magnetic moments instead of one. The concern in such a dimer for transition elements is that the electrons will antiferromagnetically couple, making the effective electron magnetic moment much smaller, the consequence of which would be a decrease in the efficiency of the metal-center-induced relaxation. However, in the present case, the relaxation efficiency is higher in the dimer, which is consistent with the general unimportance of antiferromagnetic coupling for the lanthanide complexes.

Inspection of Table I shows that neglecting special effects of the dimerization reaction leads to an intermoment distance of 2.6 Å, which is considerably shorter than expected for lanthanide complexes with water. If we assume that each proton in the dimer complex may interact with two metal centers and include a factor of 2 in the relaxation equation, then an equivalently precise fit is obtained with an intermoment distance of 3.1 Å. The correlation time for the rotation of the complex is proportional to the volume of the reorienting unit, which is larger for the dimer than the monomer. However, the correlation time for the high pH complex derived from the inflection point of the dispersion curve is somewhat shorter than those associated with the neutral pH values. This insensitivity of the inflection point to the volume of the complex would be expected if the dimer created a situation where the electron relaxation time became on the order of the rotational correlation time of the dimer. That is, where the electron relaxation time became on the order of 60 ps in the dimer.

One may anticipate that the relaxation in a many-spin system such as this one might become very complex. Indeed, we make no claim that the equations presented here account for all features of the data; however, they do account for the major qualitative features of the data and provide the basis for interpretation that is consistent with the structural chemistry of the complexes and the associated reorientational dynamics. Though caution is required, it is interesting to note that over the pH range up to 9, the data provide no additional hint of more complex behavior. Only one electron relaxation time parameter is needed to account for the shape of the dispersion profile, though it is not clear that only one such relaxation time should be sufficient.[22-26] At pH values over 9, the data are fit less well by a single Lorentzian function. This broadening could arise from a distribution of species or from a complication in the electron relaxation itself.[27,28]

Finally, we note that at pH = 1 the relaxation rate on the high-frequency side of the inflection is approximately 30% that of the low-frequency rate as predicted by Solomon's theory.[20] In all other cases, the data do not agree with the 30% prediction. Nevertheless, the relaxation dispersion profiles are well described by a Lorentzian approximation to the spectral density function, and the parameters that describe the shape and amplitude, namely the correlation time and the intermoment distance, are reasonable. In summary, these data show remarkable consistency over a broad pH range and point to possible advantages of using multimetal paramagnetic centers.

Acknowledgment. This work was supported by the National Institutes of Health, Grant GM-39309, the University of Rochester, and the Squibb Institute for Medical Research. Useful discussions with Cathy Lester, Dr. Jill Rogalskyj, Professor George McLendon, and Dr. Scott Kennedy are gratefully acknowledged.

(35) Carrington, A.; McLahlan, A. D. *Introduction to Magnetic Resonance*; Harper and Row: New York, 1967.
(36) Herz, H. G. *Water: A Comprehensive Treatise*; Franks, F., Ed.; Plenum Press: New York, 1973; Chapter 7.
(37) Lippard, S. J.; Schugar, H.; Walling, C. *Inorg. Chem.* **1967**, *6*, 1825.
(38) Banci, L.; Bencini, A.; Dei, A.; Gattesci, D. *Inorg. Chem.* **1981**, *20*, 393.
(39) Bertini, I.; Lanini, G.; Luchinat, C. *J. Magn. Reson.* **1985**, *63*, 56.
(40) Owens, Ch.; Drago, R. S.; Bertini, I.; Luchinat, C.; Banci, L. *J. Am. Chem. Soc.* **1986**, *108*, 3298.
(41) Hudson, A.; Lewis, J. W. E. *Trans. Faraday Soc.* **1970**, *66*, 1297.

Contribution from the Department of Chemistry, Gorlaeus Laboratoria, Leiden University, P.O. Box 9502, 2300 RA Leiden, The Netherlands, Anorganisch Chemisch Laboratorium, University of Amsterdam, Nieuwe Achtergracht 166, 1018 WV, Amsterdam, The Netherlands, and School of Chemical Sciences, Dublin City University, Dublin 9, Ireland

Ruthenium Compounds Containing Pyridyltriazines with Low-Lying π^* Orbitals

Ronald Hage,[†] John H. van Diemen,[†] Grant Ehrlich,[†] Jaap G. Haasnoot,*[,†] Derk J. Stufkens,[‡] Theo L. Snoeck,[‡] Johannes G. Vos,[§] and Jan Reedijk[†]

Received July 5, 1989

A number of ruthenium compounds with 5,6-dimethyl-3-(pyridin-2-yl)-1,2,4-triazine (dmpt), 5,6-diphenyl-3-(pyridin-2-yl)-1,2,4-triazine (dppt), and 3,5,6-tris(pyridin-2-yl)-1,2,4-triazine (tpt) have been prepared. The structures of the complexes have been characterized by using ^{1}H NMR spectroscopy. The two isolated geometrical isomers of $[Ru(dmpt)_3]^{2+}$ have slightly different electronic properties. The emission, resonance Raman, and electrochemical data show that the LUMO (lowest unoccupied molecular orbital) of all complexes has pyridyltriazine character. A correlation between the electrochemical and absorption/emission data has been observed.

Introduction

Ruthenium compounds with 2,2'-bipyridine (bpy) have been studied extensively because of their potential use as catalysts for the photochemical splitting of water and as redox-catalysts on polymer-modified electrodes.[1-9] Especially ruthenium compounds

[†] Leiden University.
[‡] University of Amsterdam.
[§] Dublin City University.

(1) Kalyanasundaram, K.; Gratzel, M.; Pelizetti, E. *Coord. Chem. Rev.* **1986**, *69*, 57.
(2) Seddon, E. A.; Seddon, K. R. *The Chemistry of Ruthenium*; Elsevier: Amsterdam, 1984.
(3) Meyer, T. J. *Pure Appl. Chem.* **1986**, *58*, 1193.

0020-1669/90/1329-0988$02.50/0